

# Computational Prediction of Complicated Atmospheric Motion for Spinning or non-Spinning Projectiles

Dimitrios N. Gkritzapis, Elias E. Panagiotopoulos, Dionissios P. Margaris, and Dimitrios G. Papanikas

**Abstract**—A full six degrees of freedom (6-DOF) flight dynamics model is proposed for the accurate prediction of short and long-range trajectories of high spin and fin-stabilized projectiles via atmospheric flight to final impact point. The projectile is assumed to be both rigid (non-flexible), and rotationally symmetric about its spin axis launched at low and high pitch angles. The mathematical model is based on the full equations of motion set up in the no-roll body reference frame and is integrated numerically from given initial conditions at the firing site. The projectile maneuvering motion depends on the most significant force and moment variations, in addition to wind and gravity. The computational flight analysis takes into consideration the Mach number and total angle of attack effects by means of the variable aerodynamic coefficients. For the purposes of the present work, linear interpolation has been applied from the tabulated database of McCoy's book. The developed computational method gives satisfactory agreement with published data of verified experiments and computational codes on atmospheric projectile trajectory analysis for various initial firing flight conditions.

**Keywords**—Constant-Variable aerodynamic coefficients, low and high pitch angles, wind.

## I. INTRODUCTION

**B**ALLISTICS is the science that deals with the motion of projectiles. The word ballistics was derived from the Latin "ballista", which was an ancient machine designed to hurl a javelin. The modern science of exterior ballistics [1] has evolved as a specialized branch of the dynamics of rigid bodies, moving under the influence of gravitational and aerodynamic forces and moments. Exterior ballistics existed for centuries as an art before its first beginnings as a science. Although a number of sixteenth and seventeenth century European investigators contributed to the growing body of

This work was supported in part by the Hellenic Police and Mechanical Engineering and Aeronautics Department at University of Patras.

Dimitrios N. Gkritzapis Laboratory of Firearms and Tool Marks Section, Criminal Investigation Division, First Lieutenant of Hellenic Police, Hellenic Police, 11522 Athens, Greece (corresponding author to provide phone: 0030-6948105336; e-mail: gritzap@yahoo.gr).

Elias. P. Panagiotopoulos is Postgraduate Student, Mechanical Engineering and Aeronautics Department, University of Patras (e-mail: hpanagio@mech.upatras.gr).

Dionissios.E. Margaris is assistant professor Mechanical Engineering and Aeronautics Department, University of Patras (e-mail: margaris@mech.upatras.gr).

Dimitrios G. Papanikas is professor Mechanical Engineering and Aeronautics Department, University of Patras (e-mail: papanikas@mech.upatras.gr).

renaissance knowledge, Isaac Newton of England (1642-1727) was probably the greatest of the modern founders of exterior ballistics. Newton's laws of motion established, without which ballistics could not have advanced from an art to a science.

Pioneering English ballisticians Fowler, Gallop, Lock and Richmond [2] constructed the first rigid six-degree-of-freedom projectile exterior ballistic model. Various authors have extended this projectile model for lateral force impulses [3]-[4], linear theory in atmospheric flight for dual-spin projectiles [5]-[6], aerodynamic jump extending analysis due to lateral impulsives [7] and aerodynamic asymmetry [8], instability of controlled projectiles in ascending or descending flight [9]. Costello's modified linear theory [10] has also been applied recently for rapid trajectory projectile prediction.

The present work addresses a full six degrees of freedom (6-DOF) projectile flight dynamics analysis for accurate prediction of short and long range trajectories of high spin and fin-stabilized projectiles. The proposed flight dynamic model takes into consideration the influence of the most significant force and moment variations, in addition to gravity. The applied variable aerodynamic coefficients analysis takes into consideration the variations depending on the Mach number and total angle of attack.

The efficiency of the developed method gives satisfactory results compared with published data of verified experiments and computational codes on dynamics model analysis of short and long-range trajectories of spin and fin-stabilized projectiles.

## II. PROJECTILE MODEL

The present analysis considers two different types of representative projectiles. A typical formation of the cartridge 105mm HE M1 projectile is presented in Fig. 1, and is used with various 105mm howitzers such as M49 with M52, M52A1 cannons, M2A1 & M2A2 with M101, M101A1 cannons, M103 with M108 cannon, M137 with M102 cannon as well as NATO L14 MOD56 and L5. Cartridge 105 mm HE M1 is of semi-fixed type ammunition, using adjustable propelling charges in order to achieve desirable ranges. The projectile producing both fragmentation and blast effects can be used against personnel and materials targets.

The 120 mm (Fig. 2) Mortar System provides an organic indirect-fire support capability to the manoeuvre unit commander. It is a conventional smoothbore, muzzle-loaded mortar system that provides increased range, lethality and safety compared to the World War II-vintage 4.2-inch heavy

mortar system it replaces in mechanized infantry, motorized, armored and cavalry units. A complete family of 120 mm Enhanced Mortar Ammunition is being produced by several government and commercial sources. The M933/934 high explosive round also received full materiel release and is in production. The M929 white phosphorus/smoke received full materiel release in the second quarter of 1999 and is in production. Basic physical and geometrical characteristics data of the above-mentioned 105 mm HE M1 projectile and the non-rolling, finned 120 mm HE mortar projectile illustrated briefly in Table I.



Fig. 1 105 mm HE M1 high explosive projectile

Fig. 2 The non-rolling finned 120 mm HE mortar projectile

TABLE I  
PHYSICAL AND GEOMETRICAL DATA OF 105 MM AND 120MM PROJECTILES TYPES

Characteristics	105 mm HE M1 projectile	120 mm HE Mortar projectile
Reference diameter, mm	104.8	119.56
Total length, mm	494.7	704.98
Total mass, kg	15.00	13.585
Axial moment of inertia, kg·m <sup>2</sup>	2.326·10 <sup>-2</sup>	2.335·10 <sup>-2</sup>
Transverse moment of inertia, kg·m <sup>2</sup>	2.3118·10 <sup>-1</sup>	2.3187·10 <sup>-1</sup>
Center of gravity from the base, mm	183.4	422.9

III. TRAJECTORY FLIGHT SIMULATION MODEL

A six degree of freedom rigid-projectile model [11-14] has been employed in order to predict the "free" nominal atmospheric trajectory to final target area without any control practices. The six degrees of freedom flight analysis comprise the three translation components (x, y, z) describing the position of the projectile's center of mass and three Euler angles (φ, θ, ψ) describing the orientation of the projectile body with respect to Fig. 3.

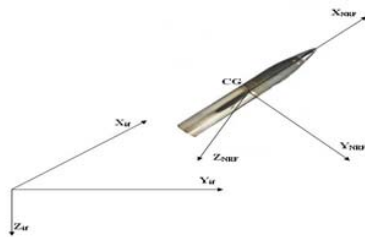


Fig. 3 No-roll (moving) and fixed (inertial) coordinate systems for the projectile trajectory analysis

Two main coordinate systems are used for the computational approach of the atmospheric flight motion. The one is a plane fixed (inertial frame, IF) at the firing site. The other is a no-roll

rotating coordinate system on the projectile body (no-roll-frame, NRF, φ = 0) with the X<sub>NRF</sub> axis along the projectile axis of symmetry and Y<sub>NRF</sub>, Z<sub>NRF</sub> axes oriented so as to complete a right hand orthogonal system.

The twelve state variables x, y, z, φ, θ, ψ, u, v, w, p, q and r are necessary to describe position, flight direction and velocity at every point of the projectile's atmospheric flight trajectory. Introducing the components of the acting forces and moments expressed in the no-roll-frame (-) rotating coordinate system in Eqs (1, 2) with the dimensionless arc length s as an independent variable, the following full equations of motion for six-dimensional flight are derived:

$$x' = D \cos \psi \cos \theta - \frac{D}{V} \sin \psi \tilde{v} + \tilde{w} \cos \psi \sin \theta \frac{D}{V} \quad (1)$$

$$y' = D \cos \theta \sin \psi + \tilde{v} \cos \psi \frac{D}{V} + \tilde{w} \sin \theta \sin \psi \frac{D}{V} \quad (2)$$

$$z' = -D \sin \theta + \frac{D}{V} \tilde{w} \cos \theta \quad (3)$$

$$\phi' = \frac{D}{V} \tilde{p} + \frac{D}{V} \tan \theta \tilde{r} \quad \theta' = \frac{D}{V} \tilde{q} \quad \psi' = \frac{D}{V \cos \theta} \tilde{r} \quad (4, 5, 6)$$

$$\tilde{u}' = -\frac{D}{V} g \sin \theta - K_1 V C_X - K_1 V C_X^2 \alpha^2 - K_1 V C_X^2 \beta^2 + \tilde{v} \frac{D}{V} \tilde{r} - \tilde{q} \frac{D}{V} \tilde{w} \quad (7)$$

$$\tilde{v}' = -K_1 C_{NA} (\tilde{v} - \tilde{v}_w) + D \frac{K_1}{2} \tilde{p} C_{MaF} \alpha - \frac{D}{V} \tilde{r} \tilde{w} \tan \theta - D \tilde{r} \quad (8)$$

$$\tilde{w}' = \frac{D}{V} g \cos \theta - K_1 C_{NA} (\tilde{w} - \tilde{w}_w) - D \frac{K_1}{2} \tilde{p} C_{MaF} \beta + D \tilde{q} + \tan \theta \frac{D}{V} \tilde{r} \tilde{v} \quad (9)$$

$$\tilde{p}' = D^5 \frac{\pi}{16 I_{XX}} \tilde{p} \rho C_{RD} \quad (10)$$

$$\tilde{q}' = 2 K_2 C_{NA} (\tilde{w} - \tilde{w}_w) L_{CGCP} + D \frac{K_2}{V} C_{MaM} \tilde{p} (\tilde{v} - \tilde{v}_w) L_{CGCM} + D^2 K_2 C_{PD} \tilde{q} + D 2 K_2 C_{OM} - \frac{D}{V} \tilde{r} \frac{I_{XX}}{I_{YY}} \tilde{p} - \frac{D}{V} \tilde{r}^2 \tan \theta \quad (11)$$

$$\tilde{r}' = -2 K_2 C_{NA} (\tilde{v} - \tilde{v}_w) L_{CGCP} + D \frac{K_2}{V} \tilde{p} C_{MaM} (\tilde{w} - \tilde{w}_w) L_{CGCM} + D^2 K_2 C_{PD} \tilde{r} - 2 D K_2 C_{OM} + \frac{D}{V} \tilde{p} \tilde{q} \frac{I_{XX}}{I_{YY}} + \frac{D}{V} \tilde{q} \tilde{r} \tan \theta \quad (12)$$

The projectile dynamics trajectory model consists of twelve highly first order ordinary differential equations, which are solved simultaneously by resorting to numerical integration using a 4th order Runge-Kutta method. In these equations, the following sets of simplifications are employed: velocity

$\tilde{u}$  replaced by the total velocity  $V$  because the side velocities  $\tilde{v}$  and  $\tilde{w}$  are small. The aerodynamic angles of attack  $\alpha$  and sideslip  $\beta$  are small for the main part of the atmospheric trajectory  $\alpha \approx \tilde{w}/V, \beta \approx \tilde{v}/V$ , the projectile is geometrically symmetrical  $I_{XY} = I_{YZ} = I_{XZ} = 0, I_{YY} = I_{ZZ}$  and aerodynamically symmetric. With the afore-mentioned assumptions, the expressions of the distance from the center of mass to the standard aerodynamic and Magnus centers of pressure are simplified

IV. INITIAL SPIN RATE ESTIMATION

In order to have a statically stable flight for spin-stabilized projectile trajectory motion, the initial spin rate  $\tilde{p}_o$  prediction at the gun muzzle in the firing site is important. According to McCoy definitions<sup>1</sup>, the following form is used:

$$\tilde{p}_o = 2\pi V_o / \eta D \text{ (rad / s)} \tag{13}$$

where  $V_o$  is the initial firing velocity (m/s),  $\eta$  the rifling twist rate at the gun muzzle (calibers per turn), and  $D$  the reference diameter of the projectile type (m). Typical values of rifling twist  $\eta$  are 1/18 calibers per turn for 105mm projectile. The 120 mm mortar projectile has uncanted fins, and do not roll or spin at any point along the trajectory.

V. COMPUTATIONAL SIMULATION

The flight dynamic models of 105 mm HE M1 and 120 mm HE mortar projectile types involves the solution of the set of the twelve first order ordinary differentials, Eqs (1-12), which are solved simultaneously by resorting to numerical integration using a 4th order Runge-Kutta method, and regard to the 6-D nominal atmospheric projectile flight.

The results give the computational simulation of the 6-D non-thrusting and non-constrained flight trajectory path for some specific spin and fin-projectiles types. Initial flight conditions for both dynamic flight simulation models with constant and variable aerodynamic coefficients are illustrated in Table II for the examined test cases.

TABLE II  
INITIAL FLIGHT PARAMETERS OF THE PROJECTILE EXAMINED TEST CASES

Initial flight data	105 mm HE M1 projectile	120 mm mortar projectile
x, m	0.0	0.0
y, m	0.0	0.0
z, m	0.0	0.0
$\phi$ , deg	0.0	0.0
$\theta$ , deg	15°, 30°, 45°, 60° and 70°	45°, 65°, and 85°
$\psi$ , deg	3.0	3.0
u, m/s	494.0	318.0
v, m/s	0.0	0.0
w, m/s	0.0	0.0
p, rad/s	1,644.0	0.0
q, rad/s	0.0	1.795
r, rad/s	3.61 and 3.64	0.0

VI. RESULTS AND DISCUSSION

The flight path trajectory motion with constant aerodynamic coefficients of the 105 mm projectile with initial firing velocity of 494 m/sec, initial yaw angle 3 degrees, rifling twist rate 1 turn in 18 calibers (1/18) and initial yaw rates 3.61 rad/s and

3.64 rad/s at 45° and 70°, respectively, are indicated in Fig. 4. The calculated impact points of the above no-wind trajectories with the proposed constant aerodynamic coefficients compared with accurately estimations of McCoy's flight trajectory analysis [1] provide basic differences for the main part of the atmospheric flight motion for the same initial flight conditions.

The mortar projectile of 120 mm diameter is also examined for its atmospheric constant flight trajectories predictions in at pitch angles of 45°, 65°, 85°, with initial firing velocity of 318 m/s, initial yaw angle 3° and pitch rate 1.795 rad/s. The impact points of the above trajectories are compared with an accurately flight path prediction with McCoy's trajectory data [1] as presented in Fig. 5.

At 45° the McCoy model for 105 mm M1 projectile, fired at sea-level neglecting wind conditions, gives a predicted range to impact of approximately 11,500 m and a maximum height at almost 3,490 m. From the results of the presented applied method, the maximum range is 11,600 m and the maximum height is almost 3,490 m, as shown in Fig. 4. Also at 70°, the predicted level-ground range of McCoy's model is 7,310 m with maximum height at about 6 km while the proposed trajectory simulation gives 7,550 m and 6,100 m, respectively.

At 45°, the 120 mm mortar projectile, fired at no wind conditions, gives a range to impact at 7,000 m with a maximum height at almost 2050 m. At 65°, the predicted level-ground range is approximately 5,320 m and the height is 3,280 m and at 85° gives 1,235m and 3,950m respectively. For the same initial pitch angles, the 120 mm mortar projectile of McCoy's data has longer range to impact points.

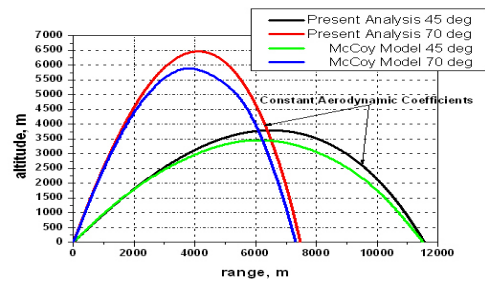


Fig. 4 Impact points and flight path trajectories with constant aerodynamic coefficients for 105 mm projectile compared with McCoy's trajectory data

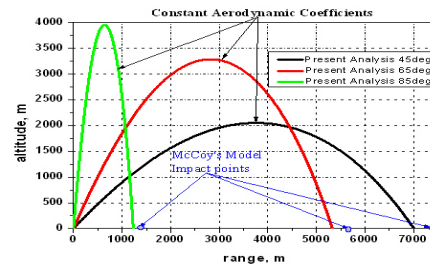


Fig. 5 Impact points and flight path trajectories with constant aerodynamic coefficients for 120 mm at quadrant elevation angles of 45°, 65° and 85° compared with McCoy's model data

In Fig. 6, the present study of the 105 mm HE M1 projectile trajectory motion with variable aerodynamic coefficients compared with McCoy's flight atmospheric model at pitch angles of 45° and 70°, provide satisfactory agreement for the same conditions. The diagram shows that the 105 mm HE M1 projectile, fired at sea-level with an angle of 45° (cyan solid line) and no wind, the predicted range to impact is 11,500 m and the maximum height is 3,490 m. At 70° (green solid line), the predicted impact point is 7,310 m, and the maximum height is slight over 6,000 m. The flight path trajectories with initial pitch angles of 15°, 30° and 60° are also shown in the same figure in comparison with the 45° and 70° flight motions. It can be stated that the maximum impact range is at 45° initial firing angle while the minimum presents at 15°.

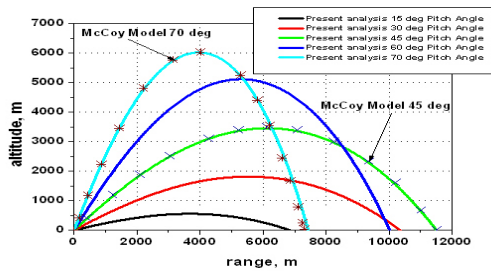


Fig. 6 Impact points and flight path trajectories with variable aerodynamic coefficients for 105 mm projectile at low and high quadrant elevation angles of 15°, 30°, 45°, 60° and 70° compared with McCoy's trajectory data

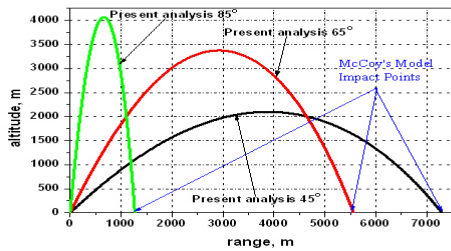


Fig. 7 Impact points and flight path trajectories with variable aerodynamic coefficients for 120 mm bullet at quadrant elevation angles of 45°, 65° and 85° compared with McCoy's data trajectory

The mortar projectile of 120 mm diameter is examined for its atmospheric variable flight trajectories predictions in Fig. 7 at low and high pitch angles of 45°, 65°, 85°, with initial firing velocity of 318 m/s, initial yaw angle 3° and pitch rate 1.795 rad/s. The impact points of the above trajectories are compared with an accurately flight path prediction with McCoy's trajectory data. At 45°, the 120 mm projectile, fired at no wind conditions gives a range to impact at 7,300 m with a maximum height at almost 2,100 m. At 65°, the predicted level-ground range is approximately 5,570 m and the height is 3,380 m and at 85° gives 1,275 and 4,070 respectively. For the same initial pitch angle, the 120 mm projectile of McCoy's data provides satisfactory agreement as 105 mm projectile.

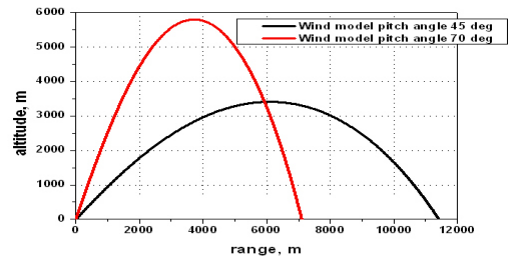


Fig. 8 Wind model path trajectories at elevation angles of 45 and 70 degrees, for 105 mm projectile

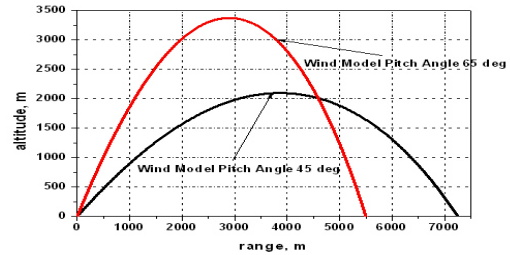


Fig. 9 Wind models of 120 mm, at pitch angles of 45 and 65 degrees

Comparative computed trajectories of the 105 mm projectile at pitch angles of 45° and 70° with a 10.0 m/s mean crosswind blowing are indicated in Fig. 8. From the computational results of the applied method at 45°, the predicted range to impact (black solid line) is almost 11,400 m and the maximum height is slightly over 3,400 m. In addition, the predicted level-ground range (red solid line) at 70° for the crosswind trajectory estimation gives the corresponding values 7,100 m and 5,800 m, respectively.

Furthermore, the computational results for 120 mm projectile at elevation angles of 45° and 65° with a 10.0 m/s mean crosswind blowing are illustrated in Fig. 9. At 45° flat-fire trajectory, the range with the wind simulation model is almost 7,250 m (black solid line) and the maximum height 2,100 m. At 65° pitch angle, the wind predicted range is 5,500 m (red solid line) and the height is almost 3,370 m.

Figs. 10 and 11 show the deflection of the flight trajectory at sea level with no-wind for the 105 mm projectile at pitch angles of 15°, 30°, 45°, 60°, 65° and for 120 mm projectile at elevation angles 45°, 65°, 85° respectively. The present analysis trajectory of the 105 mm HE M1 projectile with initial positive yaw rate 3.61 rad/s at pitch angle of 15° gives positive (right) deflection at about 146 m. On the other hand, as the initial pitch angle increases, the cross range prediction becomes negative (to the left) in comparison with the dashed reference line and increases continually at almost 700 m. Moreover, the mortar projectile of 120 mm diameter with initial firing velocity of 318 m/s, initial yaw angle 3 degrees and pitch rate 1.795 rad/s, gives always positive values of cross range 380 m, 290 m and 65 m at various low and high pitch angles, respectively.

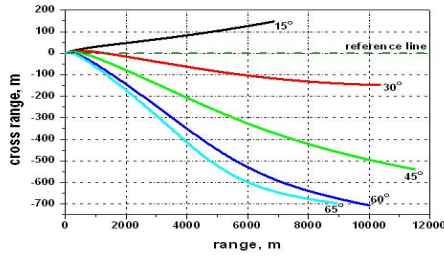


Fig. 10 Cross range versus range with variable aerodynamic coefficients for 105 mm projectile

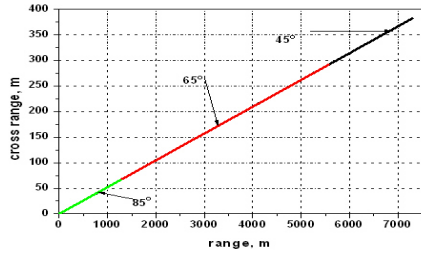


Fig. 11 Cross range computational predictions of 120 mm mortar projectile at elevation angles of 45°, 65° and 85°

VII. CONCLUSION

The complicated six degrees of freedom (6-DOF) simulation flight dynamics model is applied for the accurate prediction of short and long-range trajectories of high and low spin and fin-stabilized projectiles. It takes into consideration the Mach number and the total angle of attack variation effects by means of the variable and constant aerodynamic coefficients. The computational results of the proposed synthesized analysis are in good agreement compared with other technical data and recognized exterior atmospheric projectile flight computational models.

REFERENCES

[1] McCoy, R., *Modern Exterior Ballistics*, Schiffer, Atten, PA, 1999.  
 [2] Fowler, R., Gallop, E., Lock, C., and Richmond H., "The Aerodynamics of Spinning Shell," *Philosophical Transactions of the Royal Society of London, Series A: Mathematical and Physical Sciences*, Vol. 221, 1920.  
 [3] Cooper, G., "Influence of Yaw Cards on the Yaw Growth of Spin Stabilized Projectiles," *Journal of Aircraft*, Vol.38, No. 2, 2001.  
 [4] Guidos, B., and Cooper, G., "Closed Form Solution of Finned Projectile Motion Subjected to a Simple In-Flight Lateral Impulse," AIAA Paper, 2000.  
 [5] Costello, M., and Peterson, A., "Linear Theory of a Dual-Spin Projectile in Atmospheric Flight," *Journal of Guidance, Control, and Dynamics*, Vol.23, No. 5, 2000.  
 [6] Burchett, B., Peterson, A., and Costello, M., "Prediction of Swerving Motion of a Dual-Spin Projectile with Lateral Pulse Jets in Atmospheric Flight," *Mathematical and Computer Modeling*, Vol. 35, No. 1-2, 2002.  
 [7] Cooper, G., "Extending the Jump Analysis for Aerodynamic Asymmetry," *Army Research Laboratory*, ARL-TR-3265, 2004.  
 [8] Cooper, G., "Projectile Aerodynamic Jump Due to Lateral Impulses," *Army Research Laboratory*, ARL-TR-3087, 2003.  
 [9] Murphy, C., "Instability of Controlled Projectiles in Ascending or Descending Flight," *Journal of Guidance, Control, and Dynamics*, Vol.4, No. 1, 1981.  
 [10] Hainz, L., and Costello, M., "Modified Projectile Linear Theory for Rapid Trajectory Prediction," *Journal of Guidance, Control, and Dynamics*, Vol.28, No. 5, 2005.

[11] Etkin, B., *Dynamics of Atmospheric Flight*, John Wiley and Sons, New York, 1972.  
 [12] Joseph K., Costello, M., and Jubaraj S., "Generating an Aerodynamic Model for Projectile Flight Simulation Using Unsteady Time Accurate Computational Fluid Dynamic Results," *Army Research Laboratory*, ARL-CR-577, 2006.  
 [13] Amoruso, M. J., "Euler Angles and Quaternions in Six Degree of Freedom Simulations of Projectiles," Technical Note, 1996.  
 [14] Costello, M., and Anderson, D., "Effect of Internal Mass Unbalance on the Terminal Accuracy and Stability of a projectile," AIAA Paper, 1996.

NOMENCLATURE

$C_X$	= axial force aerodynamic coefficient
$C_{NA}$	= normal force aerodynamic coefficient
$C_{MaF}$	= magnus force aerodynamic coefficient
$C_{RD}$	= roll damping moment aerodynamic coefficient
$C_{PD}$	= pitch damping moment aerodynamic coefficient
$C_{OM}$	= overturning moment aerodynamic coefficient
$C_{MaM}$	= magnus moment aerodynamic coefficient
$C_{MaF}$	= magnus force aerodynamic coefficient
$x, y, z$	= projectile position coordinates in the inertial frame, m
$m$	= projectile mass, kg
$D$	= projectile reference diameter, m
$S$	= dimensionless arc length
$V$	= total aerodynamic velocity, m/s
$\tilde{u}, \tilde{v}, \tilde{w}$	= projectile velocity components expressed in the no-roll-frame, m/s
$\tilde{u}_w, \tilde{v}_w, \tilde{w}_w$	= wind velocity components in no-roll-body-frame, m/s
$\tilde{p}, \tilde{q}, \tilde{r}$	= projectile roll, pitch and yaw rates in the moving frame, respectively, rad/s
$\rho$	= density of air, kg/m <sup>3</sup>
$\varphi, \theta, \psi$	= projectile roll, pitch and yaw angles, respectively, deg
$\alpha, \beta$	= aerodynamic angles of attack and sideslip, deg
$g$	= gravity acceleration, m/s <sup>2</sup>
$I$	= projectile inertia matrix
$I_{XX}$	= projectile axial moment of inertia, kg-m <sup>2</sup>
$I_{YY}$	= projectile transverse moment of inertia about y-axis through the center of mass, kg-m <sup>2</sup>
$I_{XX}, I_{YY}, I_{ZZ}$	= diagonal components of the inertia matrix
$I_{XY}, I_{YZ}, I_{XZ}$	= off-diagonal components of the inertia matrix
$L_{CGCM}$	= distance from the center of mass (CG) to the Magnus center of pressure (CM) along the station line, m
$L_{CGCP}$	= distance from the center of mass (CG) to the aerodynamic center of pressure (CP) along the station line, m
$K_1, K_2$	= dimensional coefficients, $\pi \rho D^3 / 8m$ and $\pi \rho D^3 / 16I_{YY}$ , respectively
$K_y^2$	= non-dimensional transverse moment of inertia